Figure S1

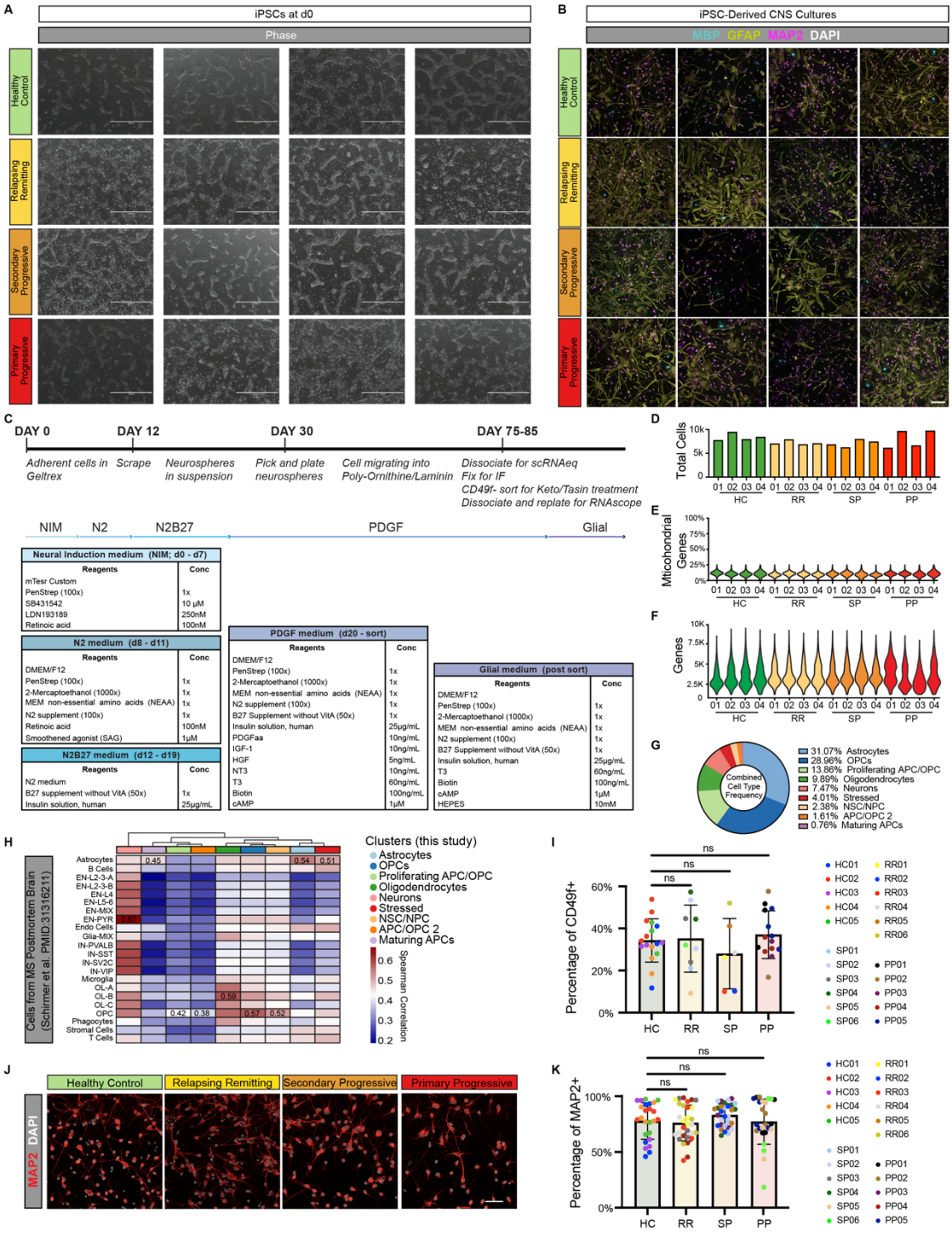

Figure S1. Characterization of iPSC-derived CNS cultures from people with MS.

(A) Representative images of undifferentiated iPSC cultures from all 16 lines used for scRNAseq analysis. Scale bar is 1mm.

(B) Representative images of iPSC-derived CNS cultures at the end of the differentiation from all 16 lines used for scRNAseq analysis. Cultures are stained for the mature oligodendrocyte marker MBP (teal), the astrocyte marker GFAP (yellow), and the neuron maker MAP2 (pink). Scale bar is 100μm.

(C) Protocol and media conditions for iPSC differentiation into CNS cells.

(D) Total cells per sample used for scRNAseq analysis.

(E) Percentage of mitochondrial genes in each scRNAseq sample.

(F) Gene counts in each scRNAseq sample.

(G) Distribution of cell types from scRNAseq analysis.

(H) Heatmap depicting the correlation between scRNAseq clusters identified in this study and cell types from scRNAseq analysis of MS brain tissue (Schirmer et al. PMID: 31316211). Spearman correlation values generated using the R package ClustifyR.

(I) Percentage of cells in healthy control (HC), relapsing remitting (RR), secondary progressive (SP), and primary progressive (PP) iPSC-derived CNS cultures that are positive for the astrocyte marker CD49f. Data is presented as mean +/- standard deviation for *n* = 5-6 lines per group (technical replicates indicated by color-coding each line) with p-values generated by one-way Anova with Dunnett's correction for multiple comparisons.

(J) Representative images of iPSC-derived neuronal cultures stained for the neuron marker MAP2 (red). Scale bar is 50μm.

(K) Percentage of cells in healthy control (HC), relapsing remitting (RR), secondary progressive (SP), and primary progressive (PP) iPSC-derived CNS cultures that are positive for the neuron marker MAP2. Data is presented as mean +/- standard deviation for *n* = 5-6 lines per group (technical replicates indicated by color-coding each line) with p-values generated by one-way ANOVA with Dunnett's correction for multiple comparisons.

Figure S2

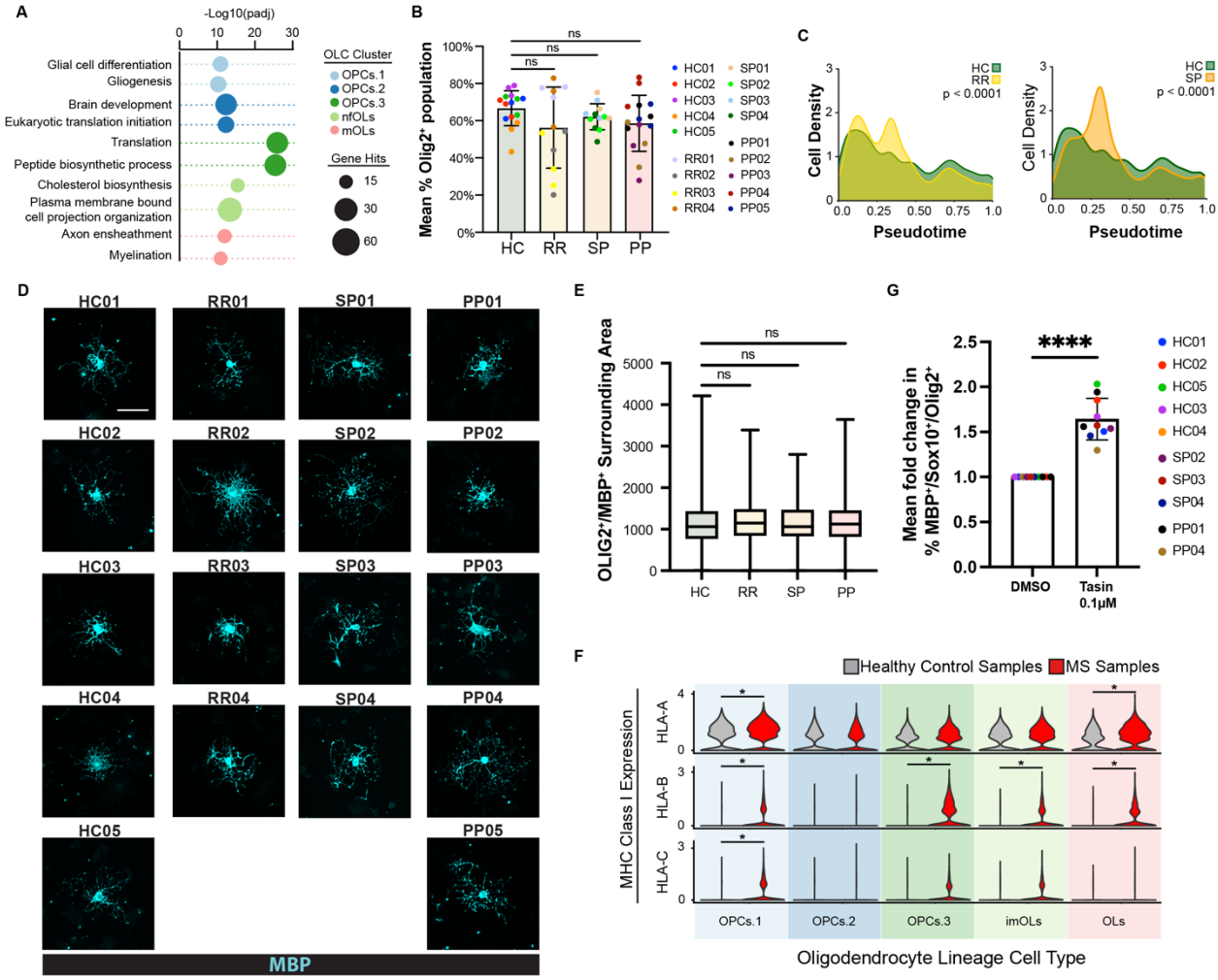

Figure S2. Characterization of iPSC-derived oligodendrocyte lineage cells from people with MS.

(A) Gene ontology analysis of genes enriched in each oligodendrocyte lineage cell type.

(B) The percentage of oligodendrocyte lineage cells in iPSC-derived cultures from healthy control (HC), relapsing remitting (RR), secondary progressive (SP), and primary progressive lines that are positive for the pan-oligodendrocyte lineage marker OLIG2. Error bars show mean ± standard deviation (n= 3 technical replicates per line for 4-5 lines per group). p-values generated by one-way ANOVA with Dunnett's correction for multiple comparisons.

(C) Cell density plot that shows the distribution of cells across the oligodendrocyte lineage trajectory from OPCs to mature oligodendrocytes for iPSC-derived cells from healthy controls (HC), relapsing remitting MS (RR), and secondary progressive MS (SP) patients. p-value generated with a two-sample Kolmogorov-Smirnov test.

(D) Representative images of mature oligodendrocytes from healthy control (HC), relapsing remitting (RR), secondary progressive (SP), and primary progressive cultures stained with the mature oligodendrocyte marker MBP. Scale bar is 50μm.

(E) Quantification of MBP^+ oligodendrocyte area for oligodendrocytes from healthy control (HC), relapsing remitting (RR), secondary progressive (SP), and primary progressive cultures. Data is presented as mean +/- standard deviation for n = 299; 150; 254; 234 cells, per respective group. p-values generated by one-way ANOVA with Dunnett's correction for multiple comparisons.

(F) Expression of MHC Class I genes in oligodendrocyte lineage cell types from healthy control and MS cultures. p-value generated by Wilcoxon ranked sum test within the Seurat R package. * $p < 0.05$.

(G) Fold-change in the percentage of MBP^+ cells in all cultures treated with vehicle (DMSO) or the oligodendrocyte enhancing compound TASIN-1 at 100nM. Data is presented as mean +/- standard deviation for n = 10 lines. p-values generated by two-way unpaired t-test.

Figure S3

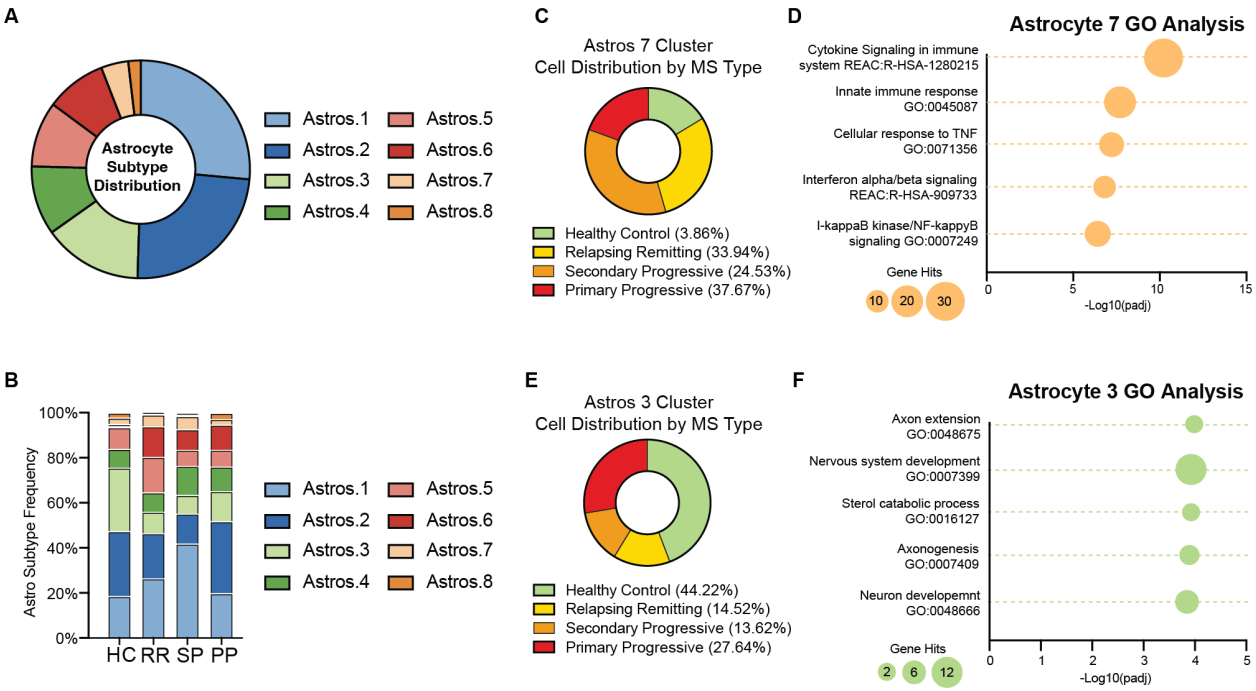

Figure S3. Reactive astrocyte subtypes in iPSC-derived astrocytes from people with MS.

(A) The proportion of each astrocyte subtype in iPSC-derived cultures from all samples.

(B) The proportion of each astrocyte subtype in iPSC-derived cultures from healthy control (HC), relapsing remitting (RR), secondary progressive (SP), and primary progressive lines. Astrocyte subclusters 6 and 7 are enriched in cultures from people with MS while astrocyte subcluster 3 is depleted in cultures from people with MS.

(C) Distribution of healthy control, relapsing remitting, secondary progressive, and primary progressive iPSC-derived astrocytes in the astrocyte subcluster 7.

(D) Gene ontology analysis of genes significantly increased in astrocytes subcluster 7 compared to all other astrocyte subclusters.

(E) Distribution of healthy control, relapsing remitting, secondary progressive, and primary progressive iPSC-derived astrocytes in the astrocyte subcluster 3.

(F) Gene ontology analysis of genes significantly increased in astrocytes subcluster 3 compared to all other astrocyte subclusters.

Figure S4

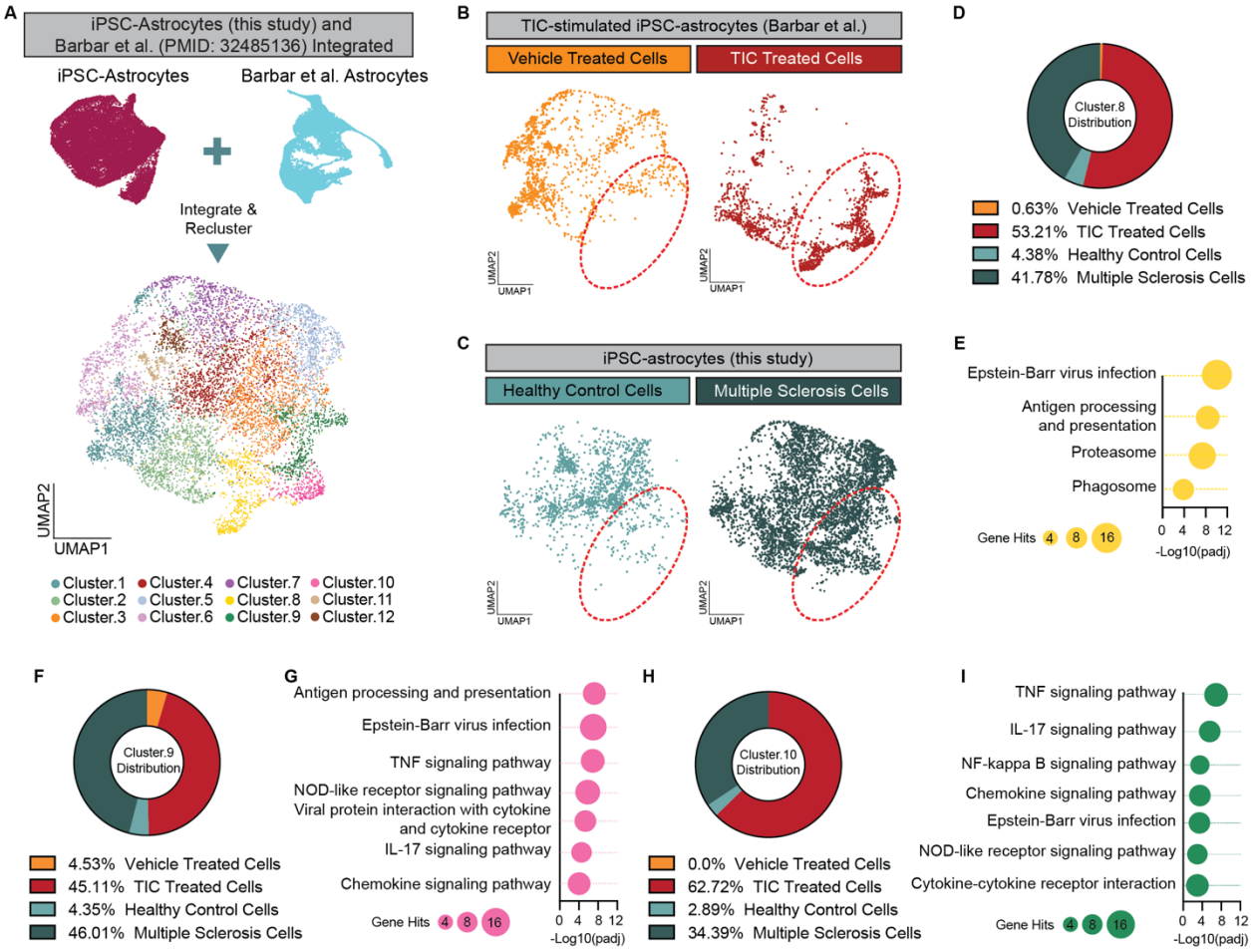

Figure S4. iPSC-derived astrocytes from people with MS share a transcriptional profile with inflammatory-driven human iPSC-derived reactive astrocytes.

(A) UMAP plot of astrocytes from this study integrated with iPSC-derived astrocytes from healthy control individuals exposed to either vehicle, or the inflammatory cytokines TNF, IL1α, and C1q (TIC) (Barbar et al. PMID: 32485136).

(B) UMAP plots showing the distribution of cells from vehicle-treated and TIC-treated iPSC-derived astrocytes. Red circle highlights Clusters 8, 9, and 10 which are enriched for iPSC-derived astrocytes exposed to TNF, IL1α, and C1q (TIC).

(C) UMAP plots showing the distribution of cells from iPSC-derived astrocytes from healthy control individuals and individuals with MS. Red circle highlights Clusters 8, 9, and 10 which are enriched for iPSC-derived astrocytes from people with MS.

(D) Distribution of vehicle-treated iPSC-derived astrocytes (yellow), TIC-treated iPSC-derived astrocytes (red), healthy control iPSC-derived astrocytes (light blue), and MS iPSC-derived astrocytes (dark blue) in Cluster 8 of the integrated data sets.

(E) Gene ontology analysis of the top 100 genes enriched in Cluster 8 of the integrated data set compared to all other clusters in the integrated data set.

(F) Distribution of vehicle-treated iPSC-derived astrocytes (yellow), TIC-treated iPSC-derived astrocytes (red), healthy control iPSC-derived astrocytes (light blue), and MS iPSC-derived astrocytes (dark blue) in Cluster 9 of the integrated data sets.

(G) Gene ontology analysis of the top 100 genes enriched in Cluster 9 of the integrated data set compared to all other clusters in the integrated data set.

(H) Distribution of vehicle-treated iPSC-derived astrocytes (yellow), TIC-treated iPSC-derived astrocytes (red), healthy control iPSC-derived astrocytes (light blue), and MS iPSC-derived astrocytes (dark blue) in Cluster 10 of the integrated data sets.

(I) Gene ontology analysis of the top 100 genes enriched in Cluster 10 of the integrated data set compared to all other clusters in the integrated data set.